Defect tolerance of brazed steel components under quasi-static and cyclic loading

M. Koster[1,a*], A. Lis[1,b], H.-J. Schindler[2,c], C. Leinenbach[1,d]

[1] Empa - Swiss Federal Laboratories for Materials Science and Technology; Joining Technologies and Corrosion; Überlandstrasse 129; 8600 Dübendorf; Switzerland

[2] Mat-Tec AG; Unterer Graben 27; 8401 Winterthur; Switzerland

[a] Michael.Koster@empa.ch (corresponding author), [b] Adrian.Lis@empa.ch,

[c] Schindler@mat-tec.ch, [d] Christian.Leinenbach@empa.ch

Keywords: Brazing, defect assessment, fatigue behavior, stress intensity factor

Abstract.
In the present work, the influence of defects on the strength of brazed joints under quasi-static and cyclic loadings was investigated. Based on experimental investigations and FE-calculations, the applicability of defect assessment procedures on brazed joints was verified for quasi static loading conditions. Further investigations in the low cycle fatigue (LCF) regime show that defects have a significant influence on the fatigue strength. Generally, defects lead to a decrease of the fatigue strength, but a direct comparison of different defects is not possible with S,N-curves. Based on the experimental results and on theoretical investigations, a procedure was developed to estimate the lifetime of defect-free and defect-containing brazed joints on the basis of the stress intensity caused by the defect. This procedure allows the direct comparison not only of defect containing, but also of defect free specimens and offers a new possibility to estimate the fatigue lifetime of brazed joints.

Greek Symbols

σ_{nom}	[MPa]	Nominal strength of the assumed defect free cross section
$\sigma_{nom(,max)}$	[MPa]	Maximum applied load on the assumed defect free cross section
σ_{UTS}	[MPa]	Ultimate tensile strength
$\sigma_{loc,max}$	[MPa]	Maximum local stress at the notch tip
$\Delta\sigma_{nom,20000}$	[MPa]	Maximum tolerable stress range to reach N_{max} failure free
ρ	[mm]	Notch radius

Latin Symbols

a	[mm]	Size of the defect
EDM	--	Electrical Discharge Machining
FE(M)	--	Finite Element (Modelling)
HT	--	High Temperature (brazing)
k	--	Dimensionless factor (to calculate $K_{I,max}$)
$K_{I(,max)}$	[MPa·m$^{0.5}$]	(Maximum) stress intesity factor
$K_{I,N}$	[MPa·m$^{0.5}$]	Notch stress intensity factor (for defect-free T-joint specimens)
LCF	--	Low Cycle Fatigue
N_{max}	--	Maximum number of loading cycles
R	--	Load ratio
W	[mm]	Specimen width

Introduction

Brazing is a method of consistent joining that provides potential for many industrial applications like the production of power electronic devices, in automotive engineering and for power generation. During the last decade, brazing has gained increasing acceptance for many seminal applications, as e.g. for space technology or for regenerative energy production [1, 2]. Compared to welding, the brazing process is characterized by relatively low process temperatures and fast processing times. Simultaneously, it allows joining small components and dissimilar materials, e.g. metals and ceramics that cannot be welded due to geometry or material combinations. With the use of advanced furnace brazing methods, as e.g. high temperature (HT) furnace brazing, joining of steel structures becomes economically more efficient [3]. HT furnace brazing is performed at elevated temperatures ($T > 900°$ C) in vacuum or with a shielding gas. HT brazed components, e.g. compressor impellers or turbine parts are usually subjected to complex loading conditions, comprising mechanical, thermal or thermo-mechanical loads.

Due to different elastic-plastic properties and geometrical effects, brazed joints form heterogeneous anisotropic systems, consisting of base material, diffusion zone and filler metal. Under mechanical loadings, constraining effects of the base material on the filler alloy lead to a triaxial stress state in the brazing zone. The resulting large hydrostatic stresses in the braze layer result in a significant change of the mechanical properties, compared to the individual joining partners [4, 5]. Furthermore, defects such as pores or incomplete gap filling may arise during brazing and act as stress concentration sites. Generally, defects can have a significant influence on the mechanical properties. To estimate the influence of defects on the joint strength under quasistatic loading conditions, procedures such as R6, BS7910 or SINTAP have been developed for welded structures and bulk materials [6 – 8]. Earlier investigations have shown that the R6-procedure can also be used for brazed joints [9]. Considering the effect of defects on the mechanical properties of brazed joints under cyclic loadings, almost no information is available in the literature [10 - 12].

The actual work shall make a contribution to estimate the influence of the specimen geometry and of defects on the strength of brazed joints. Based on experimental techniques and theoretical models, the applicability of defect assessment procedures was investigated. Further experiments in the Low Cycle Fatigue (LCF) regime were performed to establish a method to estimate the influence of different defects on the fatigue behavior.

Testing materials

For the investigations, joints consisting of the soft martensitic stainless steel AISI CA 6 NM (X3CrNiMo13-4) as a substrate material and of the gold-nickel alloy Au-18wt-% Ni as filler metal were used. The substrate material is characterized by a high corrosion resistance due to its high chrome content (Table 1) and offers potential for e.g. the production of turbo pumps or compressor impellers.

Table 1: Chemical composition of the substrate material [wt-%]

[wt-%]	**C**	**Si**	**Mn**	**Cr**	**Mo**	**P**	**Ni**
Min.	--	--	--	12	0.3	--	3.5
Max.	0.05	0.7	1.5	14	0.7	0.04	4.5

The joints were produced from plates with the dimensions 300 x 100 x 25 mm^3 by HT-furnace brazing with H_2 as a shielding gas. The brazing process was performed in an industrial shielding gas furnace (SOLO Profitherm 600) at 1020 °C for 20 minutes. After cooling down to room temperature, a subsequent annealing process was performed at 550 °C for 5.5 h.

In the scope of the experiments, standard round specimens with a diameter of 10 mm according to DIN 50125 were tested (Fig. 1a), as well as specimens with a T-joint geometry (Fig. 1 b). The T-joint respects the original geometry of the compressor impeller and takes appropriately the influence of the abrupt change of the cross section into account. Besides defect-free T-joints, also defect containing specimens were investigated to study the influence of varying defects on the quasi-static nominal strength of the assumed defect free cross section (σ_{nom}). Therefore, two different defects (straight and semi-elliptical defects) were investigated in different sizes (Fig. 1 c). The defects were introduced into the brazing zone by electrical discharge machining (EDM), using a wire with a diameter of 0.3 mm. The size of the defects was a = 0.75 mm, a = 1 mm and a = 2 mm for straight defects. Semi-elliptical defects were investigated for a = 0.75 mm, a = 1.5 mm and a = 3 mm and are characterized by the constant ratio a/c = 2/3.

Results

The performed experiments serve to investigate the influence of different specimen geometries and of defects on the joint strength. For the characterization of the substrate material, standard round specimens were tested whereas brazed joints were investigated as round shaped and as T-joint specimens. The influence of defects was examined for T-joint specimens. Based on the experimental results, FE-simulations were performed to confirm the achieved results and to characterize the influence of continuously varying defect sizes. In combination with cyclic loading experiments, the calculations could also be used to derive characteristic values to estimate the influence of a defect on the fatigue strength of brazed joints.

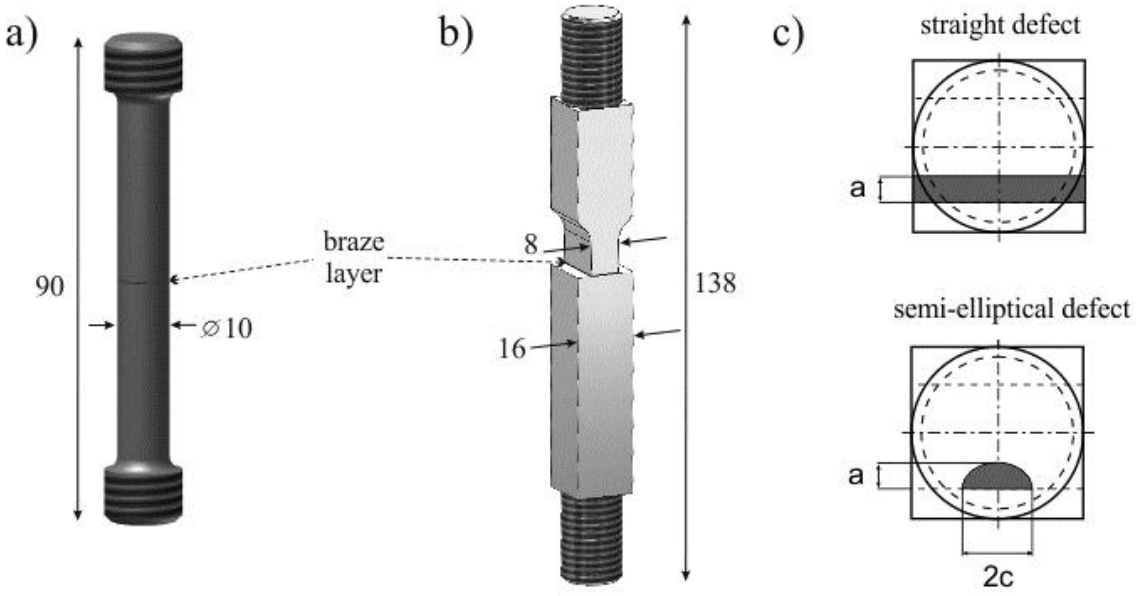

Fig. 1: Specimen geometries: (a) standard round and (b) T-joint and (c) defects

Quasistatic investigations. To determine the quasistatic properties of brazed joints and substrate material, tensile tests were performed with an electro-mechanical testing machine (Schenck Trebel RSA 250 kN). The results show that standard round specimens provide an ultimate tensile strength (σ_{UTS}) of 1224 MPa for the substrate material and a σ_{UTS} of 1084 MPa for brazed specimens. Compared to the pure filler metal that provides a σ_{UTS} of 900 MPa, the maximum tolerable loads

increase for brazed specimen. This effect is caused by constraining effects from the substrate material on the thin braze layer [4, 5].
Experiments with T-joint specimens show a slight increase of σ_{nom} to 1120 MPa compared to the round shaped specimens. This effect is caused by the T-joint geometry which leads to a triaxial stress state as a result of the change of the cross section. The multiaxial stress state restricts the deformation of the ductile braze layer and leads under quasistatic loading conditions to a decrease of the stresses in the main direction [13]. Generally, the influence of defects leads to a decrease of σ_{nom}. The decrease of the tensile strength is closely related to the size and the shape of the introduced defect. The lowest ultimate tensile strength of σ_{nom} = 453 MPa was obtained for a specimen containing a straight defect with a depth of 2 mm. The results of the tensile tests are shown in Fig. 2.

Finite element calculations. Based on the tensile tests, FE calculations were performed to numerically determine the critical limit loads and to characterize the influence of continuously varying defect sizes. With the FE software Abaqus 6.10-EF a model of the complex joint geometries was created. The 3D model consists of hexahedral brick elements with 8 nodes (C3D8R). Ideal bonding between the steel and the filler metal was assumed. Varying element sizes of 0.25 mm in the substrate material and of 0.05 mm in the brazing zone were chosen as an optimum between accuracy of simulated results and FE solution time.

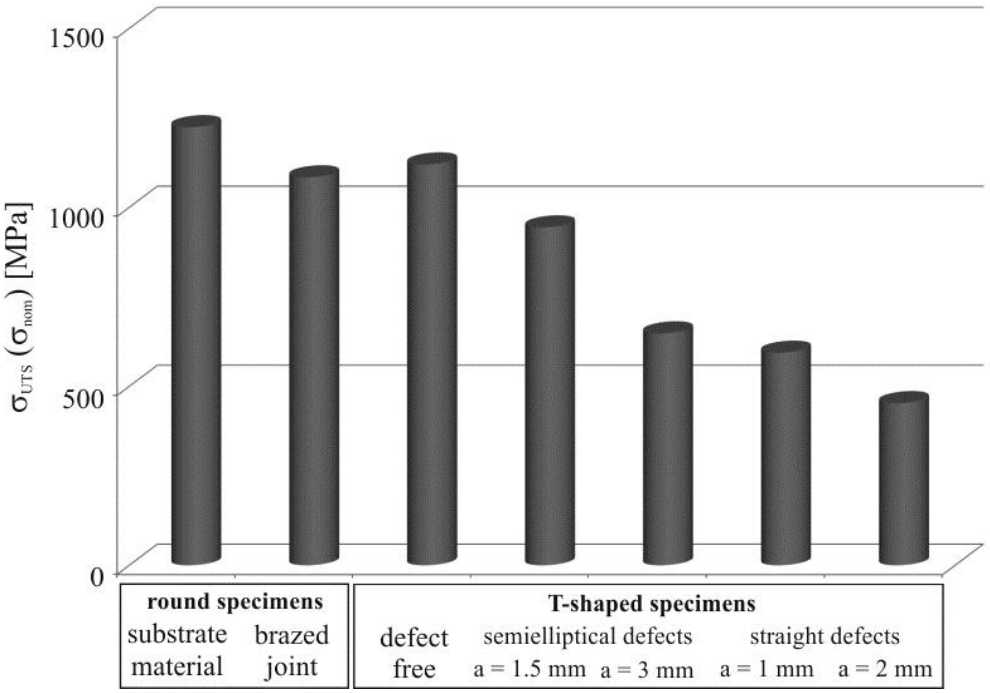

Fig. 2: Results of the tensile tests

The calculations respect the influence of the specimen geometry and the individual elastic-plastic properties of the base material and the filler alloy. The elastic-plastic deformation behavior was described by the law of Ramberg-Osgood according to Eq. 1. The material parameters of the filler metal were derived from the stress-strain curve that was determined the scope of in-situ SEM investigations [9].

$$\varepsilon = \frac{\sigma}{E} + \alpha \cdot \frac{\sigma}{E} \cdot \left(\frac{\sigma}{\sigma_y} \right)^{n-1} \tag{1}$$

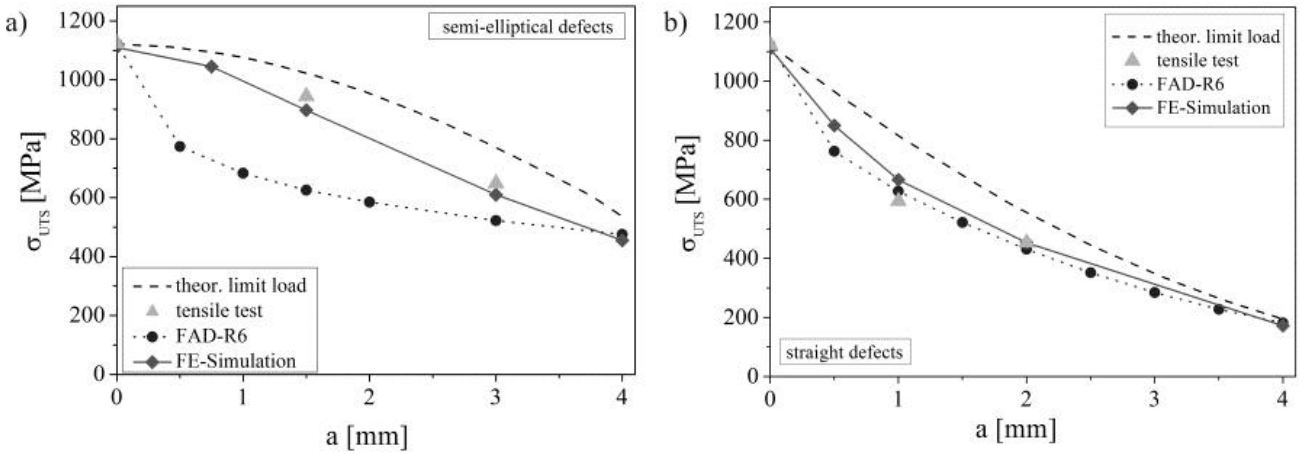

Fig. 3: Von Mises stress distribution in a T-joint with (a) semi-elliptical defects and (b) straight defects

In correlation with the experimental results, adequate failure criteria were chosen. In the present case, specimen failure was assumed to occur when the plastic strain at the interface between base material and filler metal exceeds a value of $\varepsilon_{pl,crit} = 0.015$, i.e. when the base material can be assumed to have fully plastically deformed. The results of the FE-simulations and experimental investigations are shown in Fig. 3. Furthermore, the results were compared with the limit loads according to the R6 procedure [6] and with the theoretical limit load which only takes into account the reduction of the cross section in the brazing zone due to the defects.

The results in Fig. 3 show that the experimental results and the FE-simulations are in good agreement. The theoretical limit loads exceed the experimentally determined strengths, because the stress concentration caused by the defect is not taken into account. The R6-procedure is generally applicable for the investigated joint, but it tends to provide very conservative limit loads. Fig. 3 shows that the performed FE-calculations are the most appropriate method to evaluate the influence of defects on the quasistatic joint strength. Furthermore, this method allows to calculate the limit loads for defects that continuously vary in size, shape and position, like real defects that occur during brazing.

Cyclic loading experiments. To simulate the influence of start/stop cycles on highly loaded brazed components, such as compressor impellers, fatigue experiments were performed in the LCF regime until a maximum number of loading cycles of $N_{max} = 2 \cdot 10^4$ cycles. Specimens that reached N_{max} failure-free are indicated by an arrow in Fig. 4. The tests were performed at a load ratio of R = 0.1 with a sinusoidal load at a frequency of 1 Hz. To investigate the influence of the specimen geometry on the LCF fatigue behavior, cyclic loading experiments were performed with brazed standard round specimens and with brazed T-joint specimens. The maximum tolerable stress range $\Delta\sigma_{nom,20000}$ of the round shaped specimen to reach N_{max} failure free serves as reference for the defect-free and defect containing T-joint specimens. The results of the fatigue experiments (Fig. 4) show that the specimen geometry has a significant influence on $\Delta\sigma_{nom,20000}$. Standard round shape specimens provide $\Delta\sigma_{nom,20000} = 800$ MPa while the change of the specimen geometry leads to a decrease of $\Delta\sigma_{nom,20000}$ to 450 MPa for the defect-free T-joint specimens. Defects in the braze layer lead to a further decrease of $\Delta\sigma_{nom,20000}$ with increasing defect size.The decrease of $\Delta\sigma_{nom,20000}$ seems to be more pronounced for straight defects (Fig. 4a) compared to semi-elliptical defects (Fig. 4b). A straight defect with a size of a = 2 mm leads to a decrease of $\Delta\sigma_{nom,20000}$ to 135 MPa, whereas a joint with a semi-elliptical defect of a = 3 mm provides $\Delta\sigma_{nom,20000} = 270$ MPa. The smallest semi-

elliptical defect of a = 0.75 mm exhibited the highest tolerable stress range of $\Delta\sigma_{nom,20000}$ = 360 MPa, and almost reaches $\Delta\sigma_{nom,20000}$ of the defect free T-joint specimen.

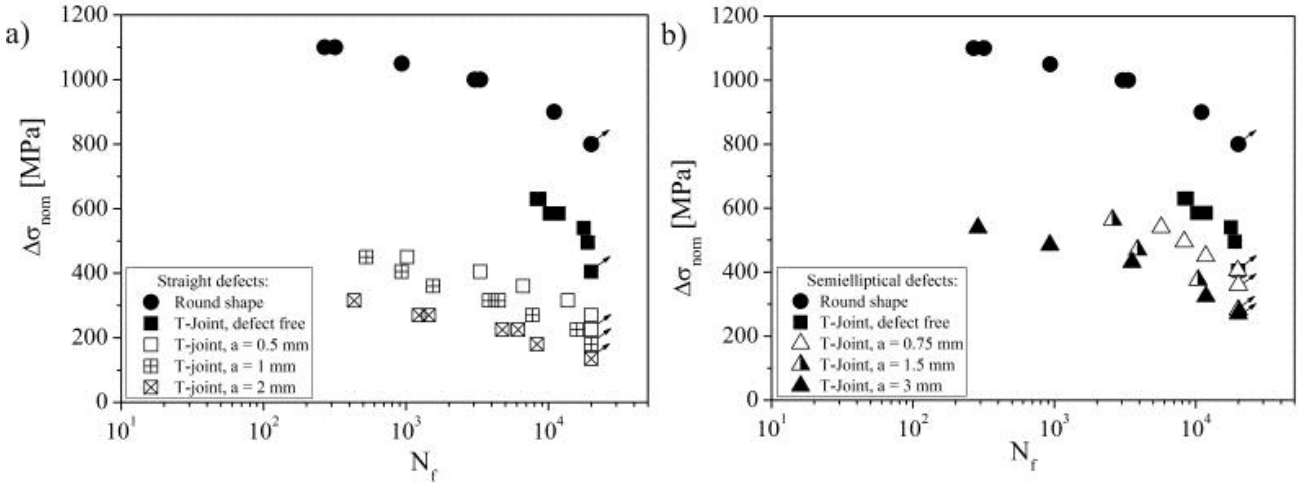

Fig. 4: Woehler curves for specimens containing (a) straight and (b) semielliptical defects

Figure 4 shows, that the size effect of identical defects can be estimated with the corresponding S,N-curve, but the direct comparison of different defects (straight defects compared with semi-elliptical defects) is not possible. Consequently, S,N curves are not applicable to estimate the influence of real defects, because real defects vary in size, shape and position within the braze layer. Therefore the actual work proposes a more general approach to estimate the influence of a defect based on the increase of the local stress concentration.

Fracture mechanics offers different models to calculate stress intensities at the tip of a crack, but the geometries of the artificial defects considered in this work as well as the geometries of characteristic brazing defects cannot be considered as cracks. Their geometries correspond to a sharp notch. The difference between a sharp notch and a crack is that it takes a certain number of loading cycles to initiate a fatigue crack from a notch. This period is defined as crack initiation period. The total fatigue life consists of the sum of crack initiation and crack propagation period. In the scope of our previous work, it could be shown that the crack propagation period can be neglected for the investigated joints [10 - 12]. Consequently, the crack initiation period that is required to initiate a fatigue crack mainly influences the fatigue lifetime. For sharp notches, a stress intensity factor K_I can be calculated with the local stress at the notch tip, $\sigma_{loc,max}$ and the notch radius ρ (Eq. 2).

$$K_I = \frac{\sigma_{loc,\max} \cdot \sqrt{\pi\rho}}{2} \tag{2}$$

Eq. 2 offers a possibility to calculate the stress intensities for the investigated joints, but it is difficult to obtain the $\sigma_{loc,max}$ experimentally. Therefore, FE-simulations were performed to calculate the resulting stress intensities [14]. For the investigated T-joint geometry, K_I was calculated as a function of the maximum applied load ($\sigma_{nom,\,max}$) and of the specimen width (W) according to Eq.3.

$$K_{I,\max} = k(a) \cdot W^{1/2} \cdot \sigma_{nom,\max} \tag{3}$$

with k as a factor considering the size and shape of the defect as well as the specimen geometry. The curse of k for straight and semi-elliptical defects as a function of the crack length a is shown in Fig. 5. With increasing crack length, the rising k-values indicate increasing stress intensities. From a crack length of a > 1 mm, the increase of k is more pronounced for straight defects, compared to semielliptical defects (Fig. 5 a).

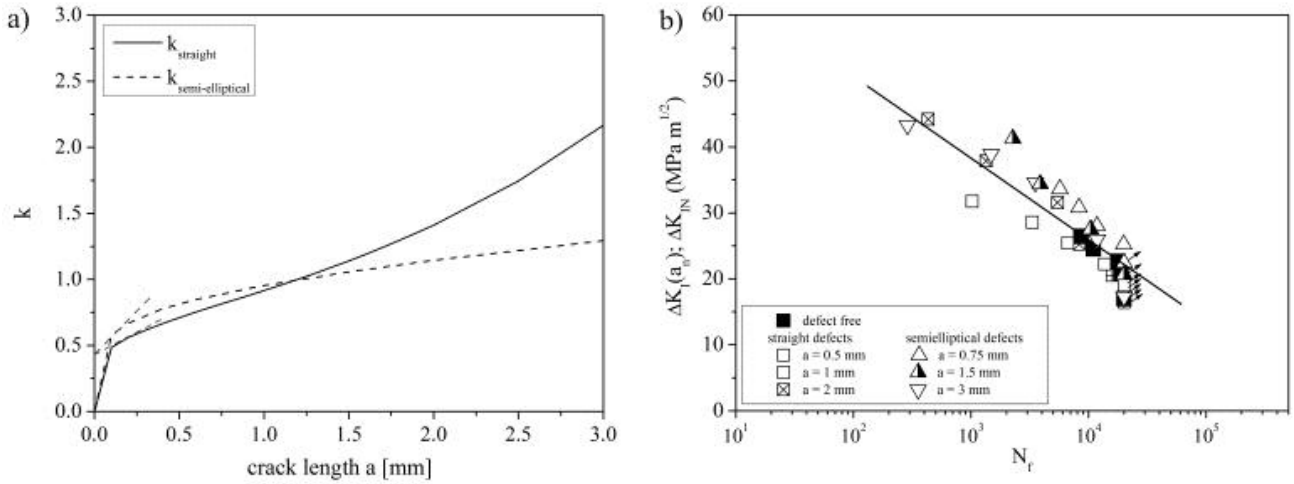

Fig. 5: (a) Dimensionless k-values for straight and semi-elliptical defects and (b) $K_{I,max}$-N curve for the investigated T-joint specimens

The plot of the resulting stress intensities in a $K_{I,max}$,N curve similar to conventional S,N-curves is shown in Fig. 5 b. In the $K_{I,max}$,N curve, the results for the specimens with different defect geometries and sizes fall into a relatively small band, indicating that the proposed method allows a direct comparison of different defect geometries. Furthermore, the proposed method allows to characterize the stress state of a defect-free T-joint by using the notch-intensity factor K_{IN}, which is defined as an extrapolation of $K_I(a)$ to a = 0 (Fig. 5 a). Mathematically, K_{IN} is obtained from Eq. 4 with k(a=0) = 0.422.

$$K_{IN} = K_I(a=0) = 0.422 \cdot \sigma_{nom} \cdot \sqrt{W} \tag{4}$$

Figure 5 b shows that the corresponding ΔK_{IN}-N-data are located well within in the scatter band of the SIF-N-curve.

Conclusions

The performed experiments show that besides the specimen geometry, also brazing defects have a significant influence on the joint strength. Considering the specimen geometry, it could be shown that the change from standard round geometry to T-joint geometry leads to an increase of σ_{UTS}. This effect occurs due to a multiaxial stress state that is caused by the specimen geometry. Consequently, σ_{UTS} of T-joint specimens exceeds the ultimate tensile strength of standard round specimens. The influence of defects generally leads to a decrease of σ_{UTS}. The results shows, that the defect assessment procedure R6 can generally be used for the estimation of defects on the quasistatic properties. For changing defect geometries, the R6 procedure deviates from the experimental results, but it generally allows a conservative estimation. The performed FE calculations seem to be most appropriate to determine the influence of defects on the quasistatic properties because they respect individual materials properties and allow investigating local effects. Simultaneously, they can be used to determine values for the estimation of a defect's influence on the fatigue life.

The fatigue experiments have shown that round shaped specimens provide the highest strengths ($\Delta\sigma_{nom,20000}$ = 800 MPa), whereas the change of the specimen geometry leads to a significant decrease of $\Delta\sigma_{nom,20000}$ to 405 MPa. The influence of defects leads to a further decrease of $\Delta\sigma_{nom,20000}$. Generally, $\Delta\sigma_{nom,20000}$ decreases with increasing defect size, but a direct comparison of different defect geometries cannot be realized with S,N-curves. Therefore, a method was developed to estimate the influence of a defect, based on the local stress intensity factor $K_{I,max}$. Combined

experimental investigations and FE-calculations allow to draw a graph of $K_{I,max}$ as a function of the numbers of cycles to failure. The good correlation between calculated and experimental results shows that the developed method allows a good estimation of the fatigue life. Furthermore, the method is also applicable for defect-free T-joint specimens and it allows evaluating the fatigue life on a unique scale.

Acknowledgements
The authors gratefully acknowledge MAN Diesel & Turbo for the funding of this project, Dr. T.A. Baser for her support during the experiments and the laboratory for Mechanical Systems and Engineering for providing the mechanical testing facilities.

References

[1]. T. Ma, M. Zeng, Y. Ji, H. Zhu and Q. Wang, in: "*Investigation of a novel bayonet tube high temperature heat exchanger with inner and outer fins"* in *Int. J. Hydrogen Energy*, Vol. 36, pp. 3757-3768, (2011).

[2]. J. Novacki and P. Swider, in: "*Producibility of brazed High-dimension Centrifugal Compressor Impellers"* in *J. Mater. Process. Technol.*, Vol. 133, pp. 174-180, (2003).

[3]. S.L. Feldbauer, in: "*Modern brazing of stainless steel"* in *Am. Weld. Soc. J.*, Vol. 10, pp. 30-33, (2004).

[4]. J. Cugnoni, J. Botsis and J. Janczak-Rusch, in: "*Size and constraining effects in lead-free solder joints"* in *Adv. Eng. Mater.*, Vol. 8, pp. 184-191, (2006).

[5]. M.E. Kassner, T.C. Kennedy and K.K. Schrems, in: "*The mechanism of ductile fracture in constrained thin silver films"* in *Acta Mater.*, Vol. 46, pp. 6445-6457, (1998).

[6]. British Energy Generation Ltd., in: "*Assessment of the integrity of structures containing defects"* in *R6-Rev. 4*, (2002).

[7]. British Standard, in: "*Guide on methods for assessing the acceptability of flaws in metallic strcutures"* in *BS 7910*, (1999).

[8]. S. Webster and A. Bannister, in: "*Structural integrity assessment procedure for Europe – of the SINTAP programme overview"* in *Eng. Fract. Mech.*, Vol. 67, pp. 481-514, (2000).

[9]. C. Leinenbach, H.J. Schindler, T. A. Baser, N. Rüttimann and K. Wegener, in: "*Quasistatic fracture behaviour and defect assessment of brazed soft martensitic stainless steel joints"* in *Eng. Failure Anal.*, Vol. 17, pp. 672-682, (2010).

[10]. C. Leinenbach, M. Koster and H.J. Schindler, in: "*Fatigue assessment of defect-free and defect containing brazed steel joints"* in *J. Mater. Eng. Perform.*, DOI: 10.1007/s11665-012-0182-7, (2012).

[11]. T.A. Baser, C. Leinenbach and H.J. Schindler, in: "*Cyclic Fracture Behaviour of Brazed Martensitic Stainless Steel Joints"* in *Proceedings of the ICF 12*, (2009).

[12]. Schindler H.J. and Leinenbach C., in: "*Mechanics of fatigue crack growth in a bonding interface"* in *Eng. Fract. Mech.*, article in press.

[13]. Irwin G.R., in: "*Analysis of stresses and strains near the end of a crack traversing a plate"* in *J. Appl. Mech.*, Vol. 24, pp. 361-364, (1957).

[14]. C. Leinenbach, H. Lehmann and H.J. Schindler, in: "*Mechanisches Verhalten und Fehlerempfindlichkeit von Hartlötverbindungen (mechanical properties and defect sensitivity of high temperature brazings)"* in MP *Materials Testing*, Vol. 49, pp. 2-9, (2007).